International Journal of Applied Earth Observation and Geoinformation 19 (2012) 104–114

Contents lists available at SciVerse ScienceDirect

International Journal of Applied Earth Observation and Geoinformation

journal homepage: www.elsevier.com/locate/jag

# Design and implementation of an algorithm for automatic 3D reconstruction of building models using genetic algorithm

Mostafa Kabolizade*, Hamid Ebadi, Ali Mohammadzadeh

*K.N.Toosi University of Technology, Faculty of Geomatics Engineering, Tehran, Iran*

ARTICLE INFO

*Article history:*
Received 10 May 2011
Accepted 15 May 2012

*Keywords:*
Building reconstruction
3D modeling
Generalization
Genetic algorithm
LiDAR

ABSTRACT

Automatic extraction and reconstruction of objects from Light Detection and Ranging (LiDAR) data and images has been a topic of research for decades. In other words, laser scanner data are powerful data source for acquisition and updating of large scale topographic maps. With this information, topographic objects like buildings, trees and the relief can be determined. The goal of this research is to extract and delineate building ground plans from LiDAR data and reconstruction of buildings in 3D space. The focus of the research lies on the different possibilities to reconstruct the building models. In this paper, a reconstruction method based on genetic algorithms (GA) is presented by optimizing height and slopes of gable roof of building models. The proposed algorithm consists of three steps; initial building boundaries are detected in the first step. Then, in extraction step, in order to improve the accuracy of detection step, initial building contours are generalized and buildings are extracted. Finally and in reconstruction step, a GA-based method is used for reconstructing the building models. Also, the method has proved to be computationally efficient, and the reconstructed models have an acceptable accuracy. Examination of the results shows that the reconstructed buildings from complex study areas that uses the proposed method have root mean square error (RMSE) of 0.1 m.



## 1. Introduction

Nowadays, automatic extraction of man-made objects such as buildings and roads in urban areas from high resolution images has become an interesting topic for photogrammetric and computer vision community. Researches in this domain has been started since late 1980s and used quite different types of source images, ranged from single intensity images, color images, laser range images to stereo and multiple images (Peng et al., 2005). Some applications include automatic information extraction from images and updating Geographic Information System (GIS) databases. On the other hand, automated reconstruction of buildings from different sources of data, particularly laser scanner data, has been one of the most challenging problems in photogrammetry and computer vision. There is an increasing demand for digital building models, which can be used in many applications including town planning, wireless telecommunication and virtual information systems for tourists and generation of 3D city models. Building reconstruction has two initial steps, which include building detection and building extraction. Many researches are presented in detection and extraction of buildings from high resolution images and LiDAR data, that some of them are Peng et al. (2005), Dash et al. (2004), Miliaresis and Nikolaos (2007). But just a few works are done in building reconstruction. Consequently, the aim of this paper is to propose a model-based reconstruction method in urban areas. Some of the related researches in this domain are represented in the next section.

## 2. Related works

Many approaches have been proposed for building detection and delineating buildings from laser scanner data. By using these methods, the outline of the ground plan could be determined. In this field, Dash et al. (2004) used height variation in the context of object periphery data to develop a method based on standard deviation in order to distinguish between trees and buildings. Sohn and Dowman (2002) employed LiDAR data to generate height data for features in an urban region. In this method, first, all features that had a certain height above ground level were identified. Then, by using the NDVI index and other information, they distinguished the buildings from other features. Miliaresis and Nikolaos (2007) proposed a new method for extracting a class of buildings by using digital elevation models (DEMs) generated by LiDAR data on the basis of geomorphometric segmentation principles. Lafarge et al. (2008) presented an automatic building extraction method that

* Corresponding author. Tel.: +98 91 63470177; fax: +98 21 88786213.
*E-mail addresses:* m_kabolizade@yahoo.com (M. Kabolizade), ebadi@kntu.ac.ir (H. Ebadi), almoh2@gmail.com (A. Mohammadzadeh).

0303-2434/$ – see front matter © 2012 Elsevier B.V. All rights reserved.
http://dx.doi.org/10.1016/j.jag.2012.05.006

involved digital elevation models based on an object approach. By using this method, a rough approximation of all relevant building footprints were first calculated from marked point processes. Kabolizade et al. (2010) presented a building detection method by using image and LiDAR data. In their method, a vegetation index with red and green bands was used for separation of buildings and trees. According to the author's knowledge, it is the first time that the roughness parameter has been used to separate trees from buildings in normalized Digital Surface Model (nDSM) data. After detecting elevated features in Digital Surface Model (DSM), the local entropy was used as roughness index to separate trees and buildings.

Initial detected contours were generalized to extract accurate contours of the detected buildings, after initial building detection. Choosing proper generalization method led to improve the building contours and would ease the subsequent building reconstruction steps by reducing the data volume. The aim of some generalization methods is representing the simplified boundary by the recursively selected extreme points. Straight lines are fitted to the original points on the boundary between two extreme points. Douglas and Peucker (1973) determined the vertices by using a decreasing of points or a geometric simplification. Simplification is carried out by fitting straight line to boundary points. Fischler and Bolles (1981) fitted straight lines to edges by least squares method. In this method, it is supposed that the buildings have simple geometric shapes. In other generalization methods (Gerke et al., 2001; Dutter et al., 2007; Shan and Sampath, 2007), general orientation and shape of buildings are used in addition to points information. In fact, a rectangle is fitted to each of the buildings and then the orientations of these rectangles represent orientations of the buildings. These types of methods lead to better performance due to the orientation information obtained from the buildings. Gerke et al. (2001) used a recursive cut of rectangles from a minimum enclosing rectangle in order to fit a rectangular outline to the jagged building outlines determined from the laser scanning data. A similar approach was realized by Dutter et al. (2007) which started with a Minimum Bounding Rectangle (MBR) and determined relevant deviations from the rectangle lines. This was done recursively in order to models different form of buildings such as L, T or U-shapes. Shan and Sampath (2007) used straight lines in the main direction of the buildings to approximate the shape. Because of the higher accuracy and better performance of second category of generalization method, the Dutter method is used in this research to generalize and extract building boundaries accurately.

The buildings boundaries extracted in previous step are used in reconstruction step. In building reconstruction, a few methods have been proposed. The existing reconstruction methods especially from LiDAR data which principally fall in two major categories: (1) the model based and, (2) data driven methods.

In the data driven methods, the roof building is partitioned to flat surfaces and a plan is fitted to each flat surface; finally the 3D model is reconstructed using these plans. In this field, Sampath and Shan (2010) presented a solution framework for the segmentation and reconstruction of polyhedral building roofs from Airborne Laser Scanner (ALS) point cloud. Kada and McKinley (2009) presented a 3D building reconstruction approach using ground plans and ALS data and used a 2D partitioning algorithm that split a building's footprint into non-intersecting, mostly quadrangular sections. A particular challenge thereby is to generate a partitioning of the footprint that approximated the general shape of the outline with less possible pieces. Once at hand, each piece forms a part of roof shape that fitted appropriately to the LIDAR points in its area and integrated well with the neighboring pieces. Kim and Shan (2011) presented a novel approach for building roof modeling from ALS data. Segmentation was performed by minimizing an energy function which formulated as multiphase level set. The roof ridges or step edges were delineated by the union of the zero level contours of the level set functions. To reconstruct a 3D roof model, roof structure points were determined by intersecting adjacent roof segments or line segments of building boundary and then connected based on their topological relations inferred from the segmentation result.

In the model based methods, reconstruction of complicated building model is carried out by use of some predefined simple primitives. As an example, Lafarge et al. (2006) started with simple rectangle primitives which were placed by using a Digital Surface Model. Afterwards a Markov Chain Monte Carlo (MCMC) simulation was employed to investigate fitness of the primitives to the buildings. Lafarge et al. (2008) also presented a new approach for building reconstruction from a single DEM. Their method treated buildings as an assemblage of simple urban structures extracted from a library of 3D parametric blocks. Dehbi and Plumer (2011) presented a novel approach to automated geometric reasoning for 3D building models. In their paper, geometric constraints are represented by multivariate polynomials whereas algebraic reasoning was based on Wu's method of pseudo-division and characteristic sets. The reasoning process was further supported by logical inference rules. Consequently, it allowed one to derive uncertain conclusions from uncertain premises. Hammoudi and Dornaika (2011) presented a model-based approach for reconstructing 3D polyhedral building models from aerial images. The 3D polyhedral models estimated directly by optimizing an objective function that is a combination of an image-based dissimilarity measure and a gradient score over several aerial images.

In the data driven methods, the performance of methods depends on the clustering method and selected thresholds by an operator. The over- and under-segmentation is the most important drawback of these methods that affect the reconstruction result. Another limitation of these methods is to determine the topologic relations among the detected roof segments (Forlani et al., 2006). On the other hand, in these methods the library of simple models are not required and these methods are more flexible.

The methods those belong to the second category are model based. These types of methods are limited by the complexity of roof shapes, since the possibility to form complex roofs is limited to the set of available primitives.

According to Forlani et al. (2006), Oude Elberink and Vosselman (2009), Sampath and Shan (2010), Verma et al. (2006), the advantage of model-based approaches is that it can always reconstruct a topologically consistent model. In contrast, in data-driven approach, the 3D model is reconstructed by assembling segmented individual roof planes.

On the other hand, one of the important deficiencies of model-based reconstruction methods is their dependencies to predefined simple models. The novelty of this paper is presenting a mode-based reconstruction approach based on genetic algorithm that has no dependency to predefined model. The proposed method can reconstruct complex building roofs using a flexible model that has no need to predefined simple primitives. For this purpose, designing a flexible model for building reconstruction and parameterizing a genetic algorithm to optimize this model in order to reconstruct complex building roofs is the aim of this paper. The proposed method in this research is a model based method that tries to solve mentioned deficiencies of former model-based methods by using genetic algorithm which can reconstruct complex building roofs by a flexible model that does not needed to predefined simple primitives.

The main aim of this research is development of a genetic algorithm for generation of a realistic 3D city model in urban areas. In the proposed algorithm, buildings are extracted and reconstructed from DSM generated by ALS data. The ALS can acquire a high density of laser points to generate the DSM of a city.

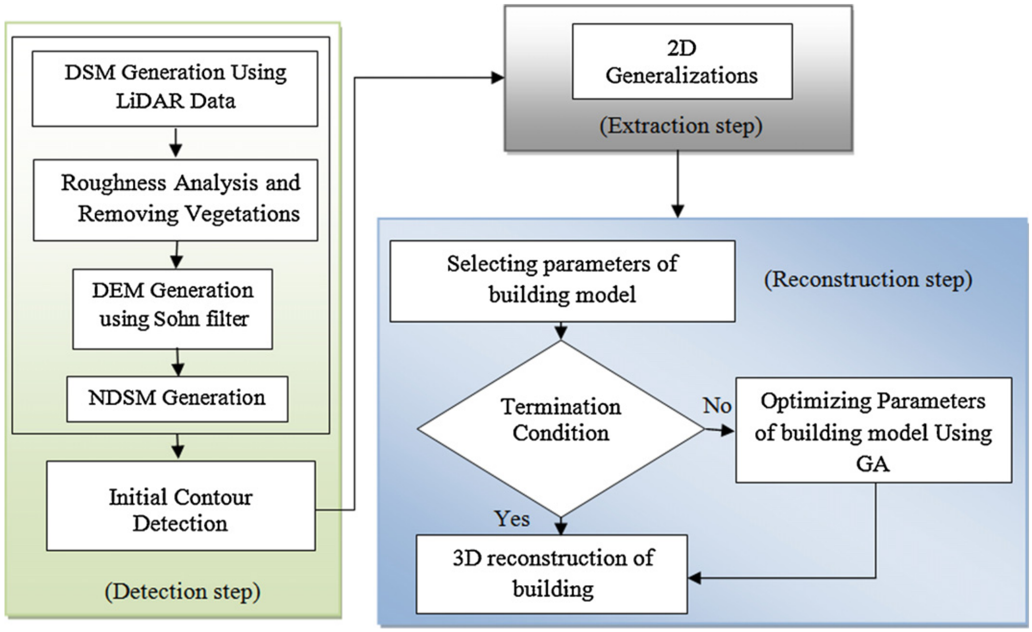


**Fig. 1.** The main steps of the proposed building reconstruction method from dense ALS data.

In the second section, the building reconstruction method which consists of selection of initial points, generalization method and reconstruction algorithm is described. In Section 4, the experimental results obtained from implementation of the proposed model are presented and numerical evaluation and limitations of the method are discussed. Finally, concluding remarks are presented in Section 5.

## 3. Building reconstruction method

Fig. 1 shows the flowchart of the proposed method for building reconstruction. This approach consists of three main steps:

(a) *Detection step*: The raw ALS point cloud has to be classified into terrain points and off-terrain points. The off-terrain points (the potential buildings) have to be aggregated to form connected building blobs. Those blobs that exceed a certain size and have certain local height and roughness characteristics are supposed to be building candidates.
(b) *Extraction step*: The outline of building is simplified. This is carried out by use of a generalization function that considers the characteristics of buildings. In this way, a meaningful 2D building shape will be produced.
(c) *Reconstruction step*: 3D model of buildings based on GA is reconstructed by use of generalized building contours and ALS data.

### 3.1. Initial contour detection

The overall aim of the detection process is to partition a DSM into regions where buildings can be constructed. This primary segmentation is carried out to reduce the dimensionality of the search space and consequently reduces the computational required time in subsequent processes. Generated DSM from ALS data is used for selection of an initial point. For the selection of initial points, the nDSM of the region is utilized (Schiewe, 2003). A DSM, generated by LiDAR data, was used to generate the DEM from LIDAR data through a filtering process. The result of this filtering was a set of points that lie on the terrain. "Sohn filter" (Sohn and Dowman, 2002) is the basis of this filtering step. Their algorithm is based on a two-step progressive densification of a triangulated irregular network (TIN). At the end of this process, points in the TIN are accepted as a representation of the bare earth, and the rest of them, as objects (Sithole, 2005). The first step of densification in this filtering approach is as same as Sohn's. Our study area was an almost flat, smooth sloped area with a few flat-roofed buildings. Because of this matter that there was no dominant topographic feature in the study area that will be discussed in Section 3, investigating the MDL (Minimum Description Length) criterion was not necessary and this step was ignored. The basic idea of using DSM in building extraction methods is that the man-made objects with different heights over the terrain can be detected by applying a threshold to the DSM. The difficulty of this process is to separate the buildings from the trees, cause both features have heights above the ground. However, their separation can be achieved by using a roughness index; for this purpose, local entropy (Eq. (1)) is used as a roughness index. Based on this index to specify trees, it is supposed that roughness in trees will be more than buildings (Fig. 2b). By using thresholding criteria, the features with higher roughness have been removed as trees and vegetations.

$$local\quad entropy = -\sum_i \sum_j p_d[i,j]\ \ln p_d[i,j] \tag{1}$$

where $p_d[i,j]$ are the gray level co-occurrence matrix array. In order to separate the above ground features from the terrain surface, a threshold value of 3 m was applied to nDSM. This threshold is arbitrary determined by the user to separate building points from remaining data (Fig. 2c). After that, a height information analysis is done to extract buildings edges from nDSM data. For this purpose, edges are detected by a canny edge detection operator after removing trees from nDSM data. Most of the edge pixels are buildings edges, and some are not, such as the edges of walls that do not belong to buildings and noisy pixels in the segmented image. Thus, the buildings boundaries should be extracted from the segmented image. Pixel connectivity is used to extract linear features. A length threshold criteria is used to remove short edges and noises. The extracted lines are not connected to each other to form a building boundary. Therefore, the edges belonging to one building are connected and then grouped to form an initial building boundary. The initial extracted building boundary is shown in Fig. 2d.

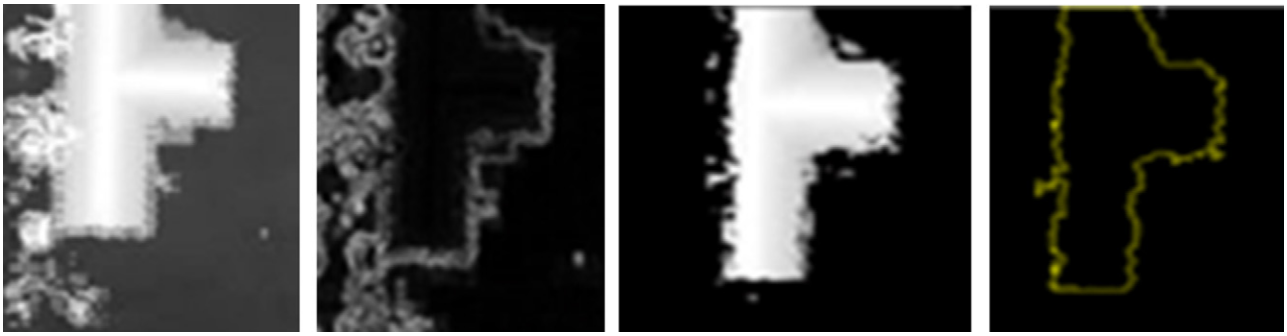

**Fig. 2.** (a) DSM, (b) roughness, (c) nDSM, (d) initial building boundary.

### 3.2. 2D generalization

As shown in Fig. 2d, straight boundaries of building polygons were zigzagged, and the corners of building polygons were closed unrealistically. Some parts of building polygons were missed, and some were extended wrongly to the background. To overcome this problem, generalization procedure proposed by Dutter et al. (2007) was used. This generalization algorithm can be divided into five major steps. The first step is to check if the point density along the building boundary is constant. Next, calculation of the major orientation of the building should be performed. This is taken from the orientation of the longer edge of the MBR. The edges of the generalized polygon are designed in such way to be parallel to one of the edges of the MBR. In the third step, split points are searched in three different levels of detail to fix the geometry of the generalized polygon as follows:

- Level 1: rectangular model.
- Level 2: “L-”, “T-” or “Z-model”.
- Level 3: “U-model”.

Afterwards, calculation of the position of the generalized edges in relation to the MBR edges is carried out. The distance of an edge from the corresponding MBR edge is the median of the distances of all points assigned to this edge from the MBR edge. The vertices of the generalized polygon are calculated by an intersection of all successive edges. In the final step, short edges are removed. This generalization algorithm has good performance in buildings with right angles.

### 3.3. 3D reconstruction of buildings

After 2D generalization of building footprint, a GA algorithm has been developed to 3D reconstruction of buildings. Since a polygon is made up of a number of sequential line segments (i.e., edges), it is intuitive to represent a polygon with the height and angle between every two adjacent edges. Thus, as illustrated in Fig. 3, an $n$-sided polygon can be established with the following parameters,

- The height of the building ($H$) from the adjacent ground surface.
- Angles $\alpha_1, \ldots, \alpha_n$ which represent orientation of the roof sides.

As it is shown in Fig. 3, a building model with complicated roof can be reconstructed by computing height and angle of each roof face with horizontal plan. The purpose is to find optimal values for these parameters and reconstruct the 3D model in order to have the most matching 3D model with the ALS data. Therefore, by using a proper optimization method, the optimum parameters values can be determined.

#### 3.3.1. Formulation of the optimization problem

The introduced variables for constructing a 3D model are part of the formulated optimization problem, which as presented below, includes variables and objective functions;

- *Variables*
  As stated before, the variables considered in this research can be categorized into two groups: height of buildings and slope angles of roof faces, which were defined in the previous section. These variables together define building model.
- *Cost functions*

An objective function is a quantified performance criterion. This function must evaluate closeness between LiDAR data and corresponding models. The objective function to be minimized in this research is sum of differences between heights in DSM and model (Eq. (2)).

$$Min: \quad index = \sum_{i=1}^{N} \left| h_i^d - h_i^m \right| \tag{2}$$

In this function $h_i^d$ is the height of a point ‘$i$’ in DSM, $h_i^m$ is the height of corresponding point in the defined model and $N$ is the number of roof points.

#### 3.3.2. Genetic algorithm

GA has proved its efficiency in dealing with different optimization problems such as the optimization of building thermal design and control, image clustering and classification as well as the design of neural network architecture. These techniques belong to a class of probabilistic search methods that strike a remarkable balance between exploration and exploitation of the search space. The optimization problem formulated in the previous section has an objective functions and continuous variables, thus continuous GA will be appropriated for such problems with parameters that have continuous and floating values. GA is initiated by selecting a population of randomly generated solutions for the considered problem.

New generations of solutions are evolved of previous generations by objective function evaluation, selection, crossover, and mutation operators.

In general, GA works with the solutions being represented by a code, rather than the initial variables. Typically, a solution is represented with a string of numbers, called chromosome. Each number represents a position that is called a gene, and the values that each gene can take are called alleles (Goldberg, 1989). Afterwards, GA evaluates the individuals in the population and then generates new (improved) solutions for the next generation. Each generation of parents will produce generation of children with an average performance better than the parent generation. The population that is chosen randomly will evolve to three operators: reproduction,

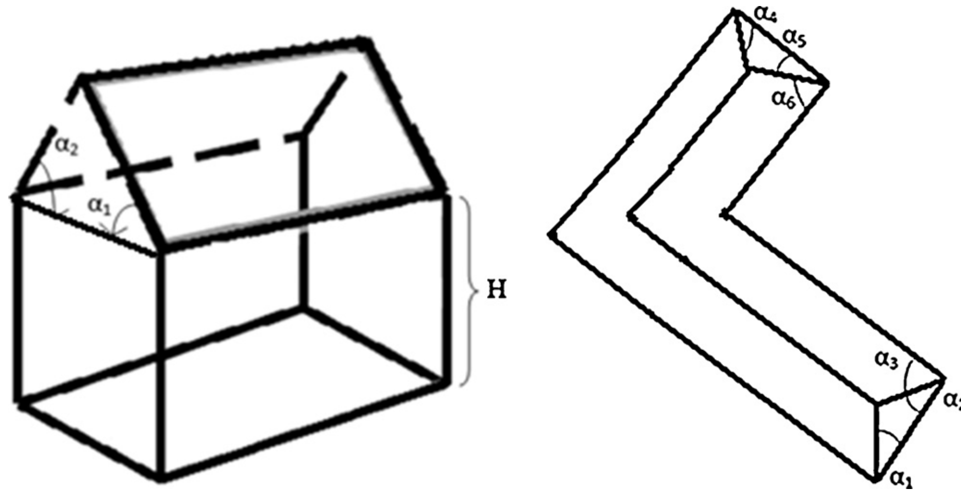


**Fig. 3.** 3D polyhedral model of a building and its parameters.

crossover and mutation. In other words, these three genetic operators take the initial population and generate successive populations that improve over time. The detailed explanations are given in the following order.

- *Encoding*: Before developing a GA, the encoding must be chosen in such a way that it will be used to represent an eventual solution of the problem by a chromosome where the value of each variable is represented by one or several genes. The quality of the algorithm depends essentially on the adopted encoding strategy and its adequacy to the used crossover and mutation operators, while respecting the nature of variables and the constraints of the problem. Since the problem variables are discrete and from different types, a real encoding is opted in order to represent the solutions by a chromosome. In this research, chromosomes with variable length have been used. The length of each chromosome is selected according to the shape of building, for example, in rectangular buildings, each chromosome consists of five gens including height of building and slopes of roof faces, while in L-shape buildings chromosomes consist of seven gens. The variation range of each parameter is chosen according to actual scales of the parameter in its nature (Fig. 4).
- *Reproduction*: For the selection process, an improved approach, known as the elitism approach is used rather than the basic one, called the wheel selection (Znouda et al., 2007). It consists of copying the best elements of the current population and inserting them into the following generation. Then it is impossible for the best element of the new generation to be worse than the one obtained in the preceding iterations. The performances of the algorithm are then greatly improved (Znouda et al., 2007). The chromosomes with the lowest cost are kept to produce the next generation, while the chromosomes with the highest cost are removed from mating pool.
- *Crossover*: Random selected pairs of chromosomes those are mated, create new ones that will be inserted in the next generation. According to the chromosomes those remained in mating pool, the parents have been selected randomly and offsprings of next generation are made using weighted mating (Eq. (3)).

$$offspring\ \ 1 = \alpha \times parent\ \ 1 + (1 - \alpha) \times parent\ \ 2 \tag{3a}$$

$$offspring\ \ 1 = \beta \times parent\ \ 1 + (1 - \beta) \times parent\ \ 2 \tag{3b}$$

In this equation $\alpha$ and $\beta$ are random numbers. All the search space is evaluated by use of weighted mating approach, and these results in an increase in the probability of converging to true optimum.
- *Mutation*: The traditional operator of mutation is replaced by the immigration procedure (Znouda et al., 2007). Instead of altering the value of one or several genes, a reduced number of new individuals are regenerated randomly. This reduces the probability of converging to local optimum. A mutation rate of 5% is chosen. The needed mutated population can be achieved by multiply the mutation rate by the total number of chromosomes.

| | | | | |
|---|---|---|---|---|
| (2-5 m) | (0°-90°) | (0°-90°) | (0°-90°) | (0°-90°) |
| 3.27 | 24.76 | 70.01 | 2.09 | 3.25 |
| ↓ | ↓ | ↓ | ↓ | ↓ |
| $H$ | $\alpha_1$ | $\alpha_2$ | $\alpha_3$ | $\alpha_4$ |

**Fig. 4.** An example of a used chromosome.

## 4. Experimental results

After extracting 2D contours of the buildings and designing appropriate GA, the proposed algorithm was implemented on two types of datasets: (a) simulated ALS data, and (b) real ALS data. In the simulated data, different types of buildings including rectangular, L, T, Z and U shapes with various sizes were designed. The roof steepness in buildings was designed in a wide range and opposite planes was designed asymmetrically. In order to assess the proposed algorithm in different conditions, the buildings were originated in different sizes and the complexity of building roofs were varied in the designed buildings.

The real ALS data from an urban area was chosen as the first case study provided by ISPRS (http://isprs.ign.fr/packages/zone1/package1_en.htm, 2010). This data includes a building with complicated shape. There are the ALS data, aerial image and reference 3D model in this dataset. The noises in this data and existing reference model let the algorithm to be assessed properly. The second real case-study is an ALS data of an urban area from west Azerbaijan Province of Iran that was scanned by use of Riegl LMS-Q560 scanner with 15 cm horizontal and 25 cm vertical nominal accuracy. Various forms of buildings with different orientations and roof shapes exist, in this study. Existence of disturbing objects such as vegetated areas and trees close to the buildings make an opportunity to test the performance and efficiency of the proposed

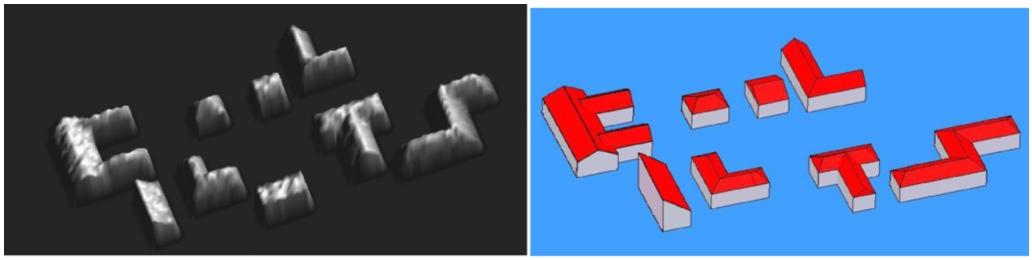

(a) (b)

**Fig. 5.** a) Simulated DSM with random noises. (b) Reconstructed DSM with different buildings' roof.

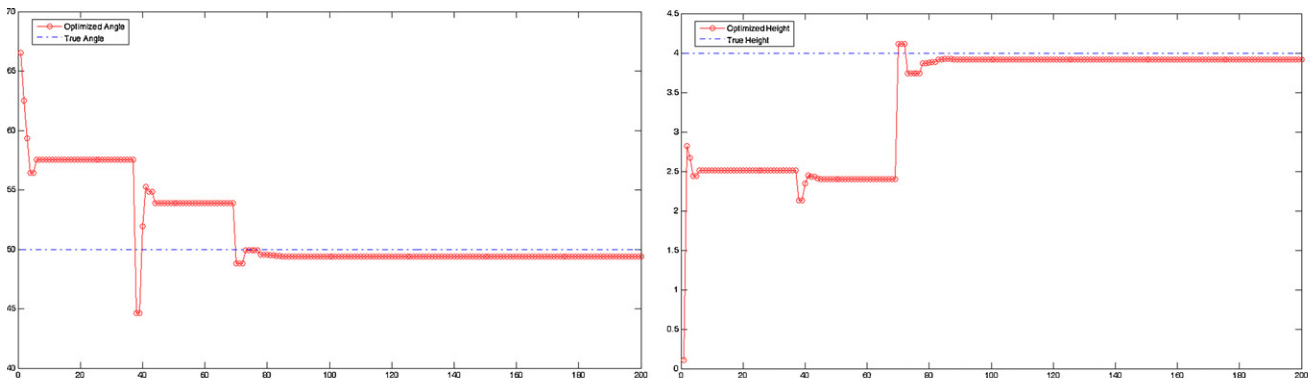


**Fig. 6.** Convergence to the optimal values of height and angle.

algorithm. The implementation results for both simulated and real data are given in the following sections.

### *4.1. Simulated ALS data*

Fig. 5(a) shows the produced simulated ALS data which consists of different types of buildings and complicated roofs. In the simulated ALS data, the true value of building height and roof angles are known. These data are used to evaluate the closeness of computed parameters using proposed method and true values. In order to better simulation of the ALS data, random noises were added to the simulated ALS points. The simulated buildings have different shapes, heights, roof steepness and sizes in order to conduct a comprehensive test of the proposed algorithm's efficiency and accuracy.

Before applying the proposed algorithm on interested buildings that appears in the image, some of the parameters need to be adjusted accordingly. The first parameter is to determine the height variation domain which is considered to be 2 m around the mean height ($h_{mean}$) of the buildings. In other words, the actual height of the building $h$ would fall in the domain of $[h_{mean} - 1 : h_{mean} + 1]$. For the second parameter, size of the initial population is set to 30. The last parameter is terminating iteration number which is set to 200.

In the developed algorithm, each chromosome represents a polyhedral and the costs of the chromosomes in each population are calculated by use of cost function of Eq. (2). Then, in the consequent iterations, new population is produced based on the reproduction, crossover and mutation those were mentioned in the previous sections. These iterations continue until reaching to the terminating criteria. It should be noted that, for proper reconstruction of buildings 'roofs, an angular threshold of ($Th_1 = 5^\circ$) has been considered, which means that the possible roof faces with angles under the $Th_1$ are assumed to be flat roofs. Additionally, a possible roof face with large angle greater than $Th_2 = 75^\circ$ would not be considered as a roof face but as a vertical face.

By use of the mentioned thresholds, the proposed method was applied on the simulated images. Fig. 6 shows the convergence of the algorithm to the optimal values of $\alpha_1$ and $H$, after 80 iterations. The speed and efficiency of the developed algorithm, depends on the population size and the maximum number of iterations. Several tests have been carried out and the results indicate that a population size of 30 up to 100 ($N < 100$) and maximum iterations of 200 up to 300 would be appropriate to achieve optimal results.

Table 1 represents the accuracies obtained by applying the proposed method on the simulated ALS data shown in Fig. 5(a). In this table, minimum difference, mean difference, maximum difference, root mean square error, total root mean square error of height differences between the laser points and the reconstructed roof planes and processing time were computed for the parameters those calculated by the algorithm and reference data.

For better interpretation of the results, one of the complex buildings was chosen as an example to analyze the performance of the method in more details. Fig. 7 shows the chosen building from the simulated data of Fig. 5(a).

As shown in Fig. 7(a), the user can discriminate 6 faces and one angle for each face, but the detected outline of the building shows the possibility of a building with 10 faces as shown in Fig. 7(b). After applying the method on the input building data based on the number of possible faces obtained from the detected building outline,

**Table 1**
Numerical results obtained by applying the proposed method on simulated data.

| | Angles of roofs (°) | Height of building ($H$) (m) |
|---|---|---|
| Minimum difference (min. diff.) | 0.03 | 0.06 |
| Mean difference (mean diff.) | 1.2 | 0.23 |
| Maximum difference (max. diff.) | 4.3 | 0.56 |
| Root mean square error (RMSE) | 0.43 | 0.17 |
| RMSE (between model and points) | | 0.28 |
| Processing time (min) | | 103 |

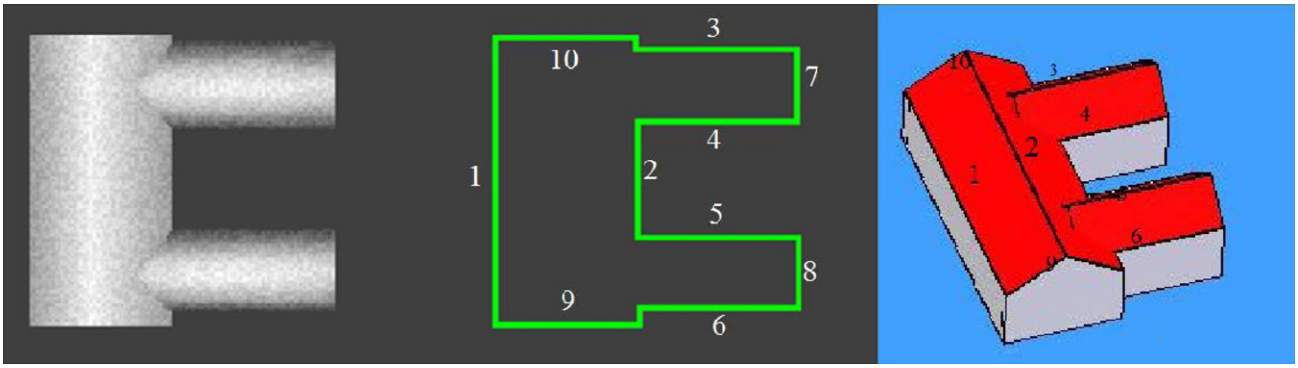


**Fig. 7.** The complex building chosen from the simulated ALS data of Fig. 5(a). Chosen building, (b) outline of the building, (c) 3D reconstructed building.

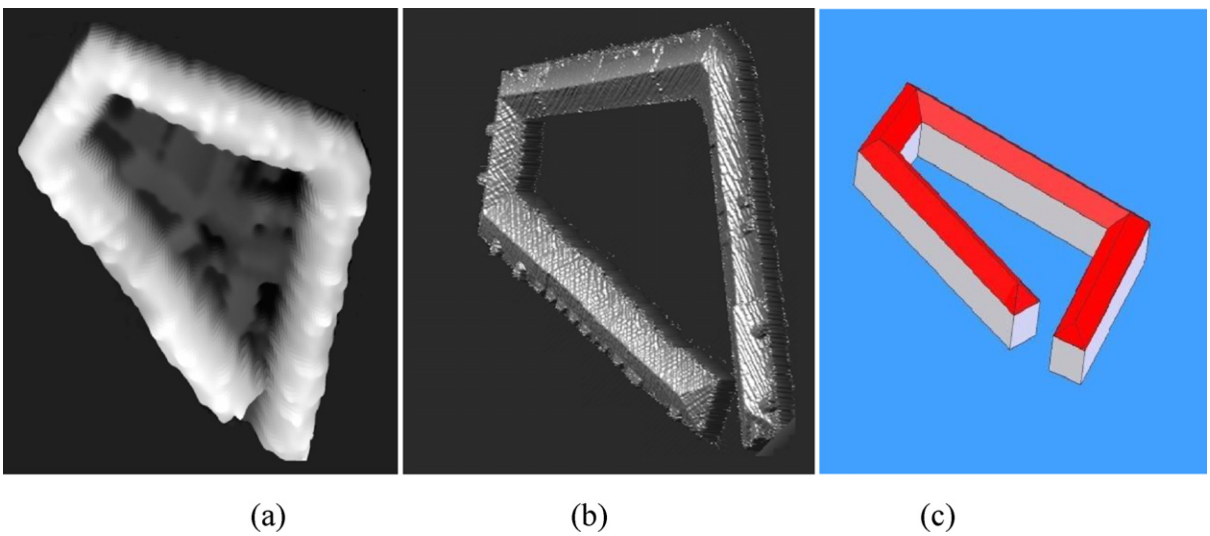

**Fig. 8.** (a) Real ALS data, (b) reference data, (c) 3D model reconstructed using the proposed method.

it is found that four faces have one 90° angle as shown in Table 2. This means that, those four faces are just vertical and thus there are six roof faces obtained by the proposed method which agree with the real number of the roof faces. It should be noted that, for a face of the roof $\sigma_h(m)$ is the standard deviation between computed roof surface and the reference data.

### *4.2. Real data (first case-study)*

As mentioned before, the first dataset was provided by ISPRS which was complex building suitable for examination of the proposed method performance. Fig. 8(a) shows the real ALS data and Fig. 8(b) shows the reference 3D model. The reconstructed

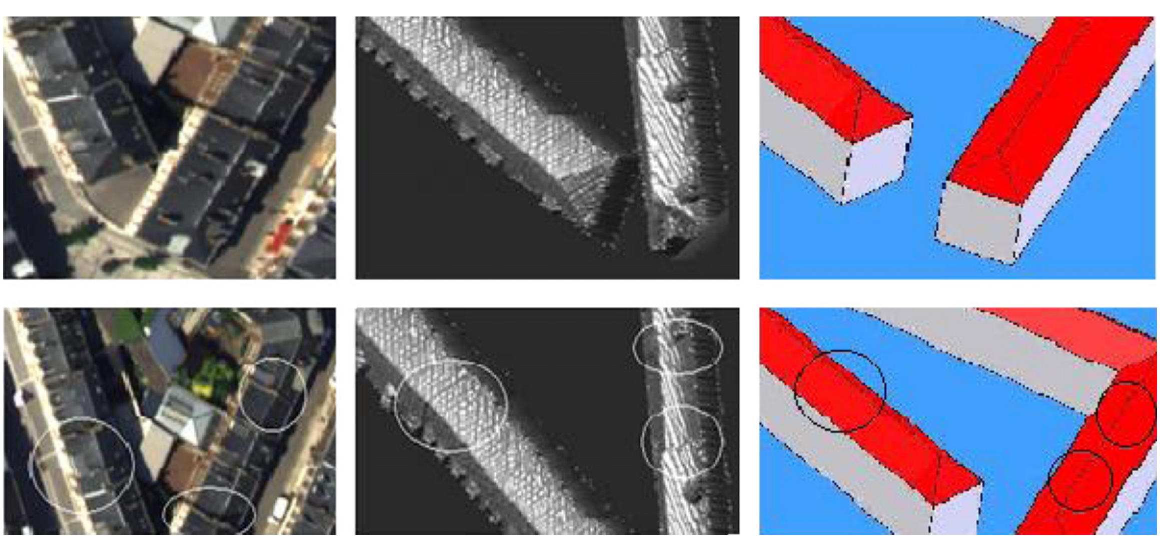

**Fig. 9.** Small deficiencies in the reconstructed roof surface, (a, d) aerial image, (b, e) reference model, (c, f) reconstructed model using proposed algorithm.

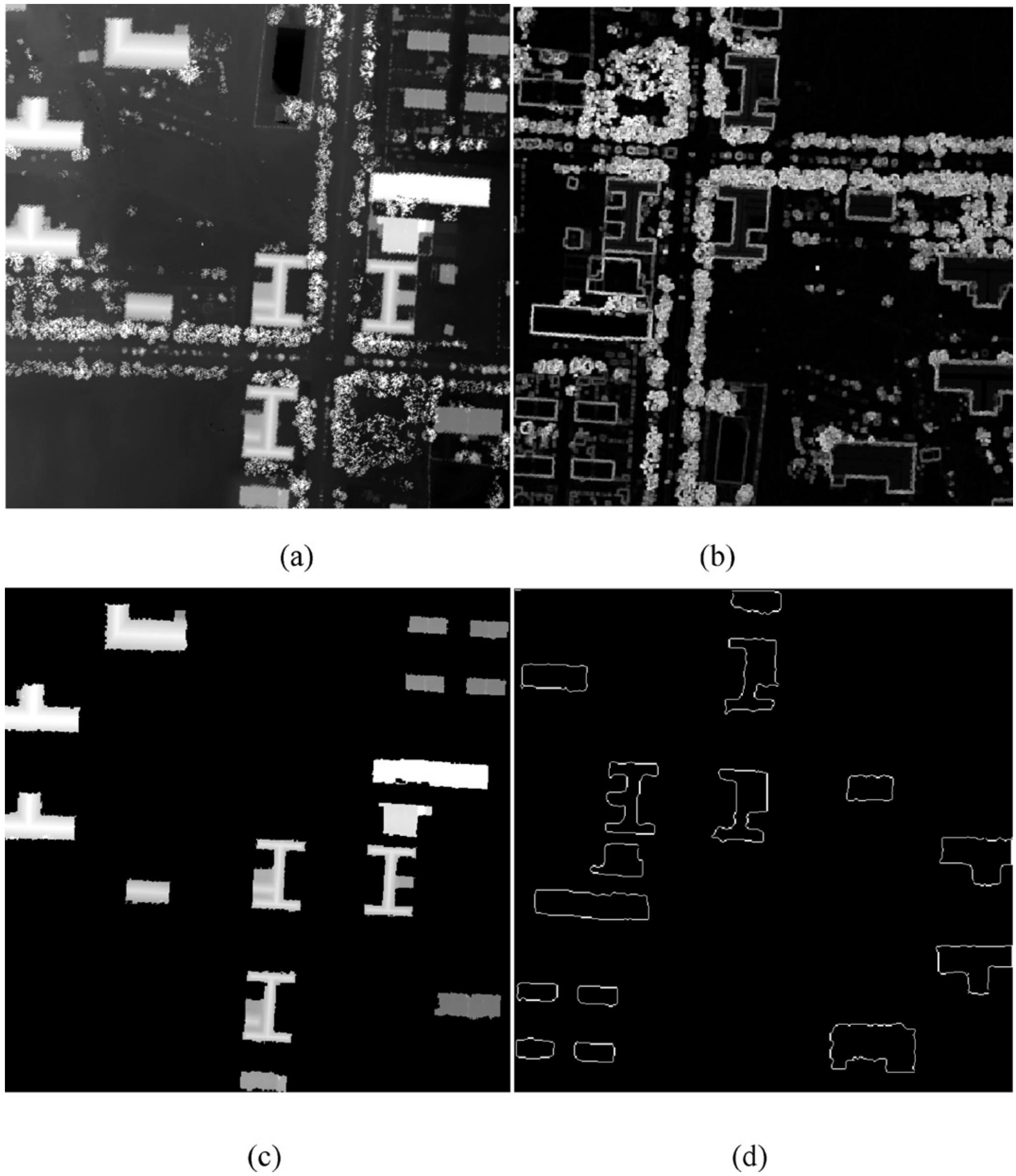

Fig. 10. (a) DSM generated by LiDAR data. (b) Roughness image. (c) In this figure, DSM objects with height less than 3 m and trees were removed. (d) Edges in LiDAR data and results of detected regions of interest.

building model obtained by the proposed method is shown in Fig. 8(c).

The accuracy assessment results obtained by comparing the reconstructed 3D building of Fig. 8(c) with the reference data of Fig. 8(b) are shown in Table 3.

**Table 2**
Calculated values of angles and height in different plans of a building in simulated data.

| Pl# | Designed angle (°) | Calculated angle (°) | $\sigma_h(m)$ |
|---|---|---|---|
| 1 | 45 | 45.12 | 0.16 |
| 2 | 32 | 30.81 | 0.33 |
| 3 | 40 | 37.93 | 0.44 |
| 4 | 50 | 49.02 | 0.31 |
| 5 | 40 | 40.80 | 0.45 |
| 6 | 50 | 51.47 | 0.29 |
| 7 | 90 | 90 | 0 |
| 8 | 90 | 90 | 0 |
| 9 | 90 | 90 | 0 |
| 10 | 90 | 90 | 0 |

The obtained results for the optimal angles and height of the building indicate the acceptable accuracy and efficiency of the proposed algorithm. By making a detailed visual comparison between the reconstructed building and reference data, still, one can find some small deficiencies in the reconstructed complex roof of the building. Fig. 9 shows two enlarged windows from the original image of Fig. 8. As shown in Fig. 9c, the proposed algorithm could not extract the details including small windows and height differences in each side of building. This algorithm fitted a 3D model

**Table 3**
Accuracy assessment for the reconstructed 3D building of the first case study.

| | Angles (°) | Height (m) |
|---|---|---|
| Min. diff. | 1.5 | 0.10 |
| Mean. diff. | 2.3 | 0.41 |
| Max. diff. | 5 | 0.72 |
| RMSE | 0.61 | 0.32 |
| RMSE (between model and points) | 0.19 | |
| Processing time (min) | 24 | |

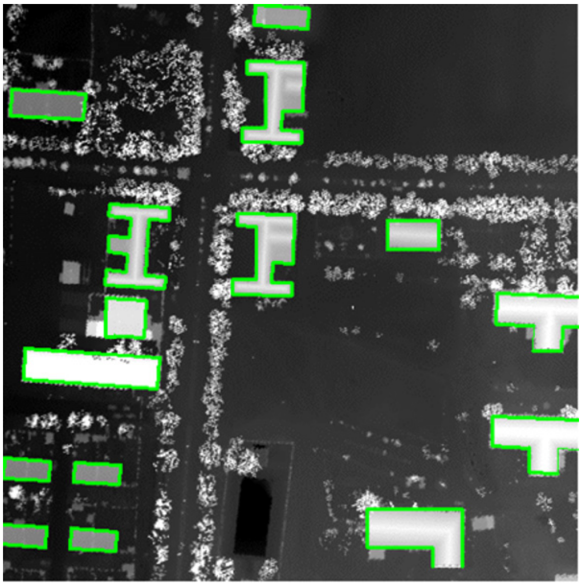

**Fig. 11.** Extracted building polygons after the generalization of building outlines.

to ALS points which eliminates the details of the real roof surface. Also, the proposed algorithm fits a steep flat plan to each face of the roof. In this case, there are vertical changes in a roof face, and the algorithm fits an optimal plan to the entire face of the roof. That is why there are some deficiencies in the faces with step heights such as shown in Fig. 9(f).

### 4.3. Real data (second case-study)

The second case study was chosen from an urban area located in Iran in west Azerbaijan Province. Fig. 10(a) shows the DSM produced from ALS point data. Reconstruction of the buildings was carried out in three steps. In the detection step, initial contour of buildings were extracted by use of the method cited in Section 3.1. For this purpose, firstly, a roughness image was produced, by use of cited roughness index (Fig. 10b). By using this image, the objects those had roughness higher than a user defined threshold were removed. In this way, the vegetations that had higher roughness were detected and removed. In the following, after calculating the nDSM (Fig. 10c) the objects with lower height (lower than 3 m) were removed and finally, as shown in Fig. 10d, by use of canny edge detection operator, the initial contour of 2D buildings were detected.

In the extraction step, in order to generalize the buildings boundaries, Dutter method was employed. This leads to the improved buildings boundaries (Fig. 11). The proposed model was evaluated by comparison with reference building models based on manual extraction. Here, the building-by-building counting method explained by McKeown et al. (2002) was applied to evaluate the performance of this proposed model (Eq. (4)).

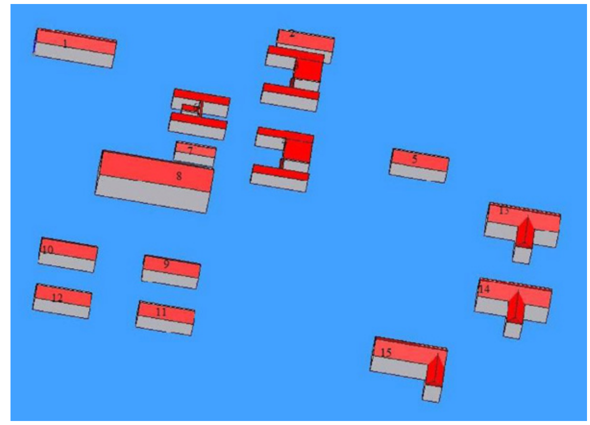

**Fig. 12.** The reconstructed 3D buildings model.

$$shape\ \ accuracy = \left(1 - \frac{|A-B|}{A}\right) \qquad (4)$$

In this equation, $A$ and $B$ are the area of a building in the ground truth data, and the area of the corresponding extracted building respectively. The results of the model evaluation by use of a building-by-building metric method showed 96% accuracy of mean shape.

In the reconstruction step, by use of the proposed method, 3D model of the buildings were reconstructed and were shown in Fig. 12. Buildings complexity affects the computational costs needed by the proposed algorithm. In the case of very complex buildings such as buildings labeled as 3 and 4 shown in Fig. 12, high population size and several iterations were required to converge to the optimal answer which is confirmed by the experimental results.

According to the complexity of the study area, in each generation 50 chromosomes were considered as GA population. Members of the first generation were selected randomly. In order to compute the cost function of each chromosome, parameters were extracted from chromosomes and 3D model were produced by use of these parameters. The cost function was calculated by separation between 3D mode and LiDAR data. Due to higher complexity of the buildings in second case study in comparison to the first one, higher number of iterations is needed to find the optimal solution with more reliability. Thus, 300 were chosen as the terminating iteration number. The accurate reconstructed 3D models which are shown in Fig. 12 show the efficiency of the method even for complex buildings. Fig. 13 shows some deficiencies in the reconstructed

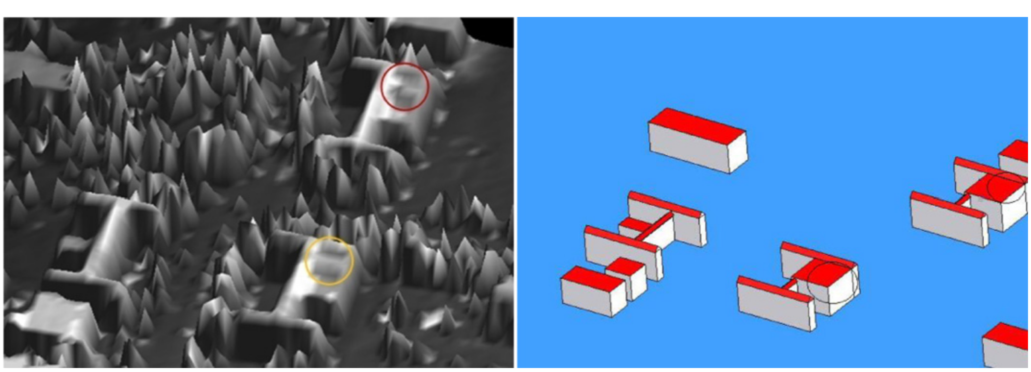

**Fig. 13.** The reconstruction errors due to difference in building roof planes.

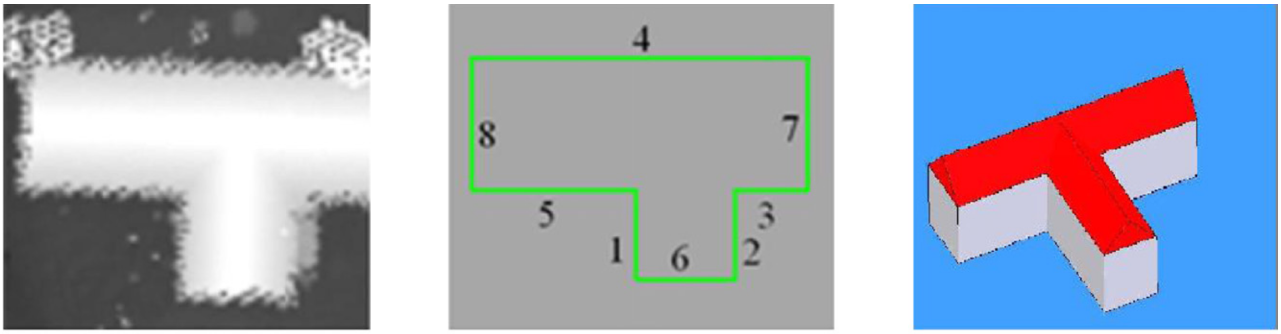


(a) (b) (c)

**Fig. 14.** The complex building chosen from the simulated ALS data of Fig. 5(a). Chosen building, (b) outline of the building, (c) 3D reconstructed building.

**Table 4**
Accuracy assessment for the reconstructed 3D building of the second case study.

| Pl# | Reference angle (°) | Calculated angle (°) | $\sigma_h(m)$ |
|---|---|---|---|
| 1 | 42.76 | 42.31 | 0.08 |
| 2 | 43.09 | 43.27 | 0.12 |
| 3 | 39.83 | 39.54 | 0.06 |
| 4 | 41.23 | 41.08 | 0.37 |
| 5 | 40.13 | 40.01 | 0.23 |
| 6 | 90 | 90 | 0 |
| 7 | 90 | 90 | 0 |
| 8 | 90 | 90 | 0 |

buildings labeled as 3, 4 and 6. These buildings have very narrow width with very few points available for roof reconstruction that results in less accurate reconstructed 3D building model.

Building 14 in Fig. 12 was chosen as the sample building to assess the accuracy and performance of the proposed method. For this purpose, an expert user fitted plans to the roof points by use of the least squares method. The manually fitted plan parameters were considered as reference data for the accuracy assessment. Fig. 14 shows the input LiDAR points for building 14 and the detected building boundary is shown in Fig. 14b. Table 4 shows the obtained parameters by the proposed method and the reference data. The small differences indicate the efficiency of the proposed method.

## 5. Summary and conclusions

In this paper, a new and sophisticated methodology is presented to reconstruct complex 3D buildings based on genetic algorithm. Designing a flexible model for building reconstruction and parameterizing a genetic algorithm to optimize this model in order to reconstruct complex building roofs, is one of the novelties of this paper. The proposed approach consists of three important steps: (1) building detection, (2) building extraction, and (3) building reconstruction. In building detection step, roughness parameter has shown to be efficient for separation of buildings from trees. Dutter method proved to be an appropriate choice for buildings boundaries extraction in the second step. In the reconstruction step as the major part of the proposed algorithm, genetic algorithm is efficiently used for optimization of a polyhedral building model with the possibility of flexible number of roof planes. The proposed method does not need any predefined simple primitives. The proposed algorithm was tested on both simulated and real ALS point cloud. Although there were complex and different buildings roofs in the simulated data, the proposed algorithm achieved RMSE of 0.43 and 0.17 for angular and height parameters of the buildings respectively. For the first real case study, the proposed algorithm obtained RMSE of 0.61 and 0.32 for angular and height parameters respectively. Effects of buildings with different shapes and gable roofs in accuracy of the reconstructed building were investigated by applying the method on the real data. Despite the difficulties related to the existence of neighboring trees close to the buildings, the method has efficiently reconstructed the buildings in all cases with RMSE of 0.1 m. Also, due to availability of acceptable number of buildings in the second case study, the 2D building extraction accuracy was studied and a shape accuracy of 96% was calculated for the extracted boundaries. Based on the obtained results, it can be concluded that the proposed method has proved its efficiency and accuracy in different building cases. It should be noted that, in very complex or very narrow buildings, there is a relative increase in the computational costs to converge to optimal buildings parameters. Future work will be directed to extract more detailed roof objects such as windows and chimneys.

## References

Dash, J., Steinle, E., Singh, R.P., Bahr, H.P., 2004. Automatic building extraction from laser scanning data: an input tool for disaster management. Advances in Space Research 33, 317–322.

Dehbi, S., Plumer, L., 2011. Automatic reasoning for geometric constraints in 3D city modelswith uncertain observation. ISPRS Journal of Photogrammetry and Remote Sensing 66, 177–187.

Douglas, D., Peucker, T., 1973. Algorithms for the reduction of the number of points required to represent a digitized line or its caricature. The Canadian Cartographer 10 (2), 112–122.

Dutter, M., Hollaus, M., Pfeifer, N., 2007. Generalization of building footprints derived from high Resolution remote sensing data. Diploma Thesis. TU Vienna.

Elberink, S.O., Vosselman, G., 2009. Building Reconstruction by Target Based Graph Matching on Incomplete Laser Data: Analysis and Limitation. Sensors 8, 6101–6118.

Fischler, M.A., Bolles, R.C., 1981. Random sample consensus: a paradigm for model fitting with applications to image analysis and automated cartography. Communications of the ACM 24, 381–395.

Forlani, G., Nardinocchi, C., Scaioni, M., Zingaretti, P., 2006. Complete classification of raw Lidar data and 3D reconstruction of buildings. Pattern Analysis and Applications 8, 357–374.

Gerke, M., Heipke, C., Straub, B., 2001. Building extraction from aerial imagery using a generic scene model and invariant geometric moments. In: Proceedings of the IEEE/ISPRS Joint Workshop on Remote Sensing and Data Fusion over Urban Areas, pp. 85–89.

Goldberg, D.E., 1989. Genetic Algorithm in Search, Optimization and Machine Learning. Addison-Wesley.

Hammoudi, K., Dornaika, F., 2011. A featureless approach to 3D polyhedral building modeling from aerial images. Sensors 11, 228–259.

Kabolizade, M., Ebadi, H., Ahmadi, S., 2010. An improved snake model for automatic extraction of buildings from urban aerial images and LiDAR data. Computers, Environment and Urban Systems 34, 435–441.

Kada, M., McKinley, L.,2009. 3D building reconstruction from LiDAR based on a cell decomposition approach. In: CMRT09, vol. XXXVIII, Part 3/W4. IAPRS.

Kim, K., Shan, J., 2011. Building roof modeling from airborne laser scanning data based on level set approach. ISPRS Journal of Photogrammetry and Remote Sensing 66, 484–497.

Lafarge, F., Descombes, X., Zerubia, J., Deseilligny, M., 2006. An automatic building reconstruction method: a structural approach using high resolution satellite images. In: Proceedings of ICIP, pp. 1205–1208.

Lafarge, F., Descombes, X., Zerubia, J., Deseilligny, M., 2008. Structural approach for building reconstruction from a single DSM. IEEE Transactions on Pattern Analysis and Machine Intelligence (PAMI) 32, 135–147.

McKeown, D.M., Bulwinkle, T., Cochran, S., Harvey, W., McGlone, C., Shufelt, J.A., 2002. Performance evaluation for automatic feature extraction. International Archives of Photogrammetry Remote Sensing 33 (Part B2), 379–394.

Miliaresis, G., Nikolaos, K., 2007. Segmentation and object based classification for the extraction of the building class from LIDAR DEMs. Computers & Geosciences 33, 1076–1087.

Peng, J., Zhang, D., Liu, Y., 2005. An improved snake model for building detection from urban aerial images. Pattern Recognition Letters 26, 587–595.

Sampath, A., Shan, J., 2010. Segmentation and reconstruction of polyhedral building roofs from aerial LiDAR point clouds. IEEE Transactions on Geoscience and Remote Sensing 48 (3), 1554–1567.

Schiewe, J., 2003. Integration of multi-sensor data for landscape modeling using a region-based approach. ISPRS Journal of Photogrammetry and Remote Sensing 57, 371–379.

Shan, J., Sampath, A., 2007. Urban Terrain and Building Extraction from Airborne LiDAR Data. CRC Press.

Sithole, G., 2005. Segmentation and classification of airborne laser scanner data (Ph.D. dissertation), in Technical University of Delft, The Netherlands.

Sohn, G., Dowman, I.J., 2002. Terrain surface reconstruction by the use of tetrahedron model with the MDL criterion. International Archives of Photogrammetry, Remote Sensing and Spatial Information Sciences 34 (Part 3), 336–344.

Znouda, E., Ghrab-Morcos, N., Hadj-Alouane, A., 2007. Optimization of Mediterranean building design using genetic algorithms. Energy and Buildings 39, 148–153.